Low-cost GNSS antennas in precise positioning: a focus on multipath and antenna phase center models

G. Krzan, K. Dawidowicz, J. Paziewski
Institute of Geodesy, University of Warmia and Mazury in Olsztyn, Poland
ul. Oczapowskiego 1, 10-720 Olsztyn
grzegorz.krzan@uwm.edu.pl

EUREF Symposium 2024, 5th – 7th June, Barcelona, Catalonia, Spain

Introduction

The rapid growth of the GNSS equipment market has put affordable receivers and antennas capable of receiving satellite signals into the hands of users. High positioning accuracy, previously achievable only with high-grade devices, is becoming possible with low-cost ones. However, simplifications in the design of these devices, intended to reduce the manufacturing cost, affect their capabilities. This study analyzes the positioning accuracy that may be achieved with recent low-cost antennas. We put particular stress on investigating the susceptibility of such antennas to the multipath effect and implications from the quality of the antenna phase center models. The positioning performance is assessed by employing the Precise Point Positioning method with the integer ambiguity resolution of phase observations. The results obtained with three low-cost antennas are validated against three high-grade antennas. We reveal a two-to threefold decrease in positioning performance with low-cost antennas compared to high-quality equipment. However, positioning accuracy increased when a low-cost antenna with a phase correction model was used, particularly for the eastern component of coordinate bias. In addition, a significant susceptibility of low-cost antennas to the multipath effect was confirmed, especially for GPS L2 and Galileo E5a signals.

Data and Method

A set of three antennas such as U-blox ANN-MB-00, Tallysman TW7972, and ELT0149, supporting quad constellations was proposed to analyze the feasibility of using low-cost GNSS antennas for precision geodetic applications (Fig.1). In addition, two surveying-grade antennas and one geodetic choke-ring antenna were employed to provide benchmark solutions. The antennas are also characterized by different information on antenna phase center offset and variations (Tab 2). For the ELT0149, there is no information on both phase center offset and variation. For U blox ANN-MB-00, the only available information is up PCO for GPS L1 and L2 signals. The Tallysman TW7972 antenna is the only one among the tested that has almost complete information regarding PCC. In the study, we used two units of TRM105000.10, Tallysman TW7972, U-blox ANN-MB-00 antenna models, and single units of ELT0149 and TRM159900.00 NONE. Each tested antenna was connected to the Trimble Alloy receivers. The antennas were collocated during the experiment as they were placed on a rigid beam with two antenna mounting points. The beam was placed on the roof of a residential building.
The GNSS data were processed in static and kinematic PPP mode with phase ambiguity resolution (PPP-AR), using PRIDE PPP-AR 2.2 software (Tab. 1). We investigate the result of the static solution derived from a processing of 16-hour long dataset processing for each day of data collection and the coordinate time series obtained in a kinematic solution with an interval of 5 s. The processing was performed in two variants: using GPS-only (G) or multi-constellation observations from GPS, GLONASS, Galileo, and BDS (GREC). We utilized the type-mean PCCs included in the IGS14_2196.atx file for professional surveying antennas used as benchmarks. For the Tallysman TW7972 antenna, the PCCs provided by the manufacturer were used, as well as PCO for U-blox ANN-MB-00. For ELT0149other low-cost antennas, zero PCCs were assumed, as no correction models are available (Fig. 2).

Tab. 1. Detailed parameters of solutions

Parameter	Setting
GNSS constellations	G or GREC
Observations	IF linear combination of dual-frequency signals from quad constellations
Stochastic modeling	a priori noise of pseudorange and phase: 0.30 m and 0.01 cycle
Solution type	PPP with ambiguity resolution, static (16 h) and kinematic (5 s interval)
Elevation angle	10°
Orbits, clocks, earth rotation parameters	Wuhan University rapid products (WUM) (Guo et al. 2016)
Differential code bias (DCB)	WUM
PCC model	IGS14_2196 for geodetic-grade antennas (type-mean), Tallysman TW7971 PCC model (type-mean) U-blox ANN-MB-00 PCO (type-mean) Zero PCC for ELT0149
Ocean loading model	FES2004
Tidal displacements	IERS Conventions 2010
Troposphere delay handling	Saastamoinen model with Global Pressure and Temperature (GPT) and Global Mapping Function (GMF) estimated every hour; priori constraint of ZTD and process noise: 0.20 m
Horizontal troposphere gradient handling	Estimated every 2 hours (piece-wise constant); priori constraint of HTG: 0.005 m
Ionospheric delay handling	1^{st} order eliminated with IF linear combination, higher orders neglected
Ambiguity resolution method	Wide-lane/Narrow-lane

Fig. 1. GNSS antennas used in the experiment: ELT0149 (left), U-blox ANN-MB-00 (middle), and Tallysman TW7972 (right). High-grade antennas are given in the bottom row: JAVGRANT-G3T (left), TRM105000.10Trimble Zephyr 3 Rover (middle), and TRM159900.00Trimble Choke-ring (right)

Tab. 2. Antennas used in the study and their PCO for GPS signals.

Antenna model	Serial no.	GPS L1 PCO [mm]			GPS L2 PCO [mm]		
		N	E	U	N	E	U
TRM159900.00 NONE	6126333759	0.61	0.08	114.07	0.25	0.52	123.95
TRM105000.10 NONE #1	3121102632	0.43	0.00	61.66	-0.47	2.66	56.54
TRM105000.10 NONE #2	61053R0021	0.43	0.00	61.66	-0.47	2.66	56.54
U-blox ANN-MB-00 #1	AGA556022-S0-A24	-	-	8.90	-	-	7.60
U-blox ANN-MB-00 #2	AGA556022-S0-A9	-	-	8.90	-	-	7.60
Tallysman TW7972 #1	20210910	0.86	-1.13	10.34	-0.59	2.34	9.95
Tallysman TW7972 #2	20210630	0.86	-1.13	10.34	-0.59	2.34	9.85
ETL0149	-	-	-	-	-	-	-
JAVGRANT-G3T NONE	01348	1.22	0.42	50.28	-3.17	1.22	46.83

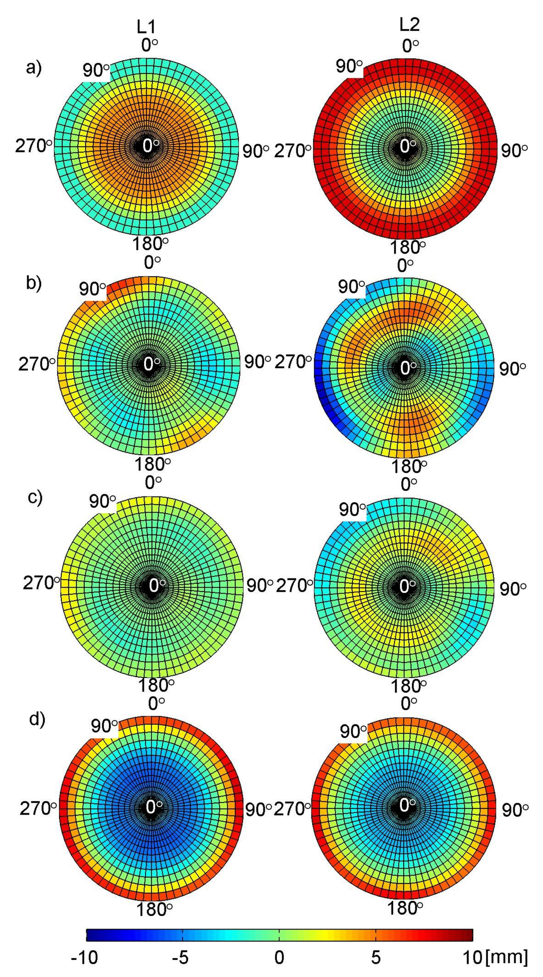

Fig. 2. Antenna PCV patterns: a) Tallysman TW7972, (b) JAVGRANT-G3T, c) TRM105000.10, d) TRM159900.00.

Tab. 3. Differences in the number of recorded carrier phase observations on mounting points 1 and 2. Positive values indicate that more observations were recorded on point 1.

DOY	Mounting point #1	Mounting point #2	GPS		GLONASS		Galileo		Beidou	
			L1C	L2X	L1P	L2C	L1X	L5X	L2I	L6I
77	U-blox ANN-MB-00 #1	U-blox ANN-MB-00 #2	-1%	-1%	-2%	-1%	2%	-2%	6%	9%
78	TRM105000.10 NONE #1	TRM105000.10 NONE #2	0%	0%	-1%	-1%	0%	0%	1%	2%
79	U-blox ANN-MB-00 #2	ELT0149	-1%	-1%	6%	4%	0%	4%	-3%	-3%
80	U-blox ANN-MB-00 #2	TRM159900.00 NONE	2%	1%	4%	2%	13%	11%	6%	-3%
81	U-blox ANN-MB-00 #1	TRM159900.00 NONE	2%	0%	4%	0%	11%	8%	8%	-8%
82	TRM105000.10 NONE #2	TRM159900.00 NONE	2%	2%	7%	6%	11%	10%	9%	10%
83	U-blox ANN-MB-00 #2	JAVGRANT-G3T NONE	-1%	-2%	-1%	-7%	1%	-2%	2%	-18%
84	U-blox ANN-MB-00 #1	JAVGRANT-G3T NONE	-1%	-1%	0%	-4%	0%	-2%	2%	-18%
85	Tallysman TW7972 #1	JAVGRANT-G3T NONE	0%	-1%	1%	-1%	0%	-2%	4%	-18%
86	Tallysman TW7972 #1	ELT0149	0%	1%	1%	2%	2%	6%	7%	-9%
87	Tallysman TW7972 #1	TRM159900.00 NONE	2%	2%	5%	4%	14%	11%	10%	-7%
88	Tallysman TW7972 #1	Tallysman TW7972 #2	0%	0%	-1%	1%	2%	2%	2%	-6%
89	Tallysman TW7972 #1	U-blox ANN-MB-00 #2	0%	1%	0%	1%	2%	2%	7%	1%

Differences in the number of recorded carrier phase observations

The differences between the number of recorded observations when the same antennas were on mounting points 1 and 2 in almost all cases do not exceed 2% (Tab. 3). The exception is Beidou signals, when low-cost antennas were operating on both points - then the difference reached 6-9%. Similar differences also occurred when different antennas worked on the points. The reason is most likely that the Beidou B1-2 and B3 signals associated with L2I and L6I carrier phases are not listed as supported by the low-cost antenna as well as JAVGRANT-G3T specifications. For GPS signals for each pair of antennas, the differences in the number of recorded observations did not exceed 2%. For the other systems, noticeable differences can be seen when the TRM159900.00 antenna was operating on one of the points. The choke-ring design of this antenna, which is meant to filter reflected signals from low elevation angles, probably resulted in fewer observations recorded.

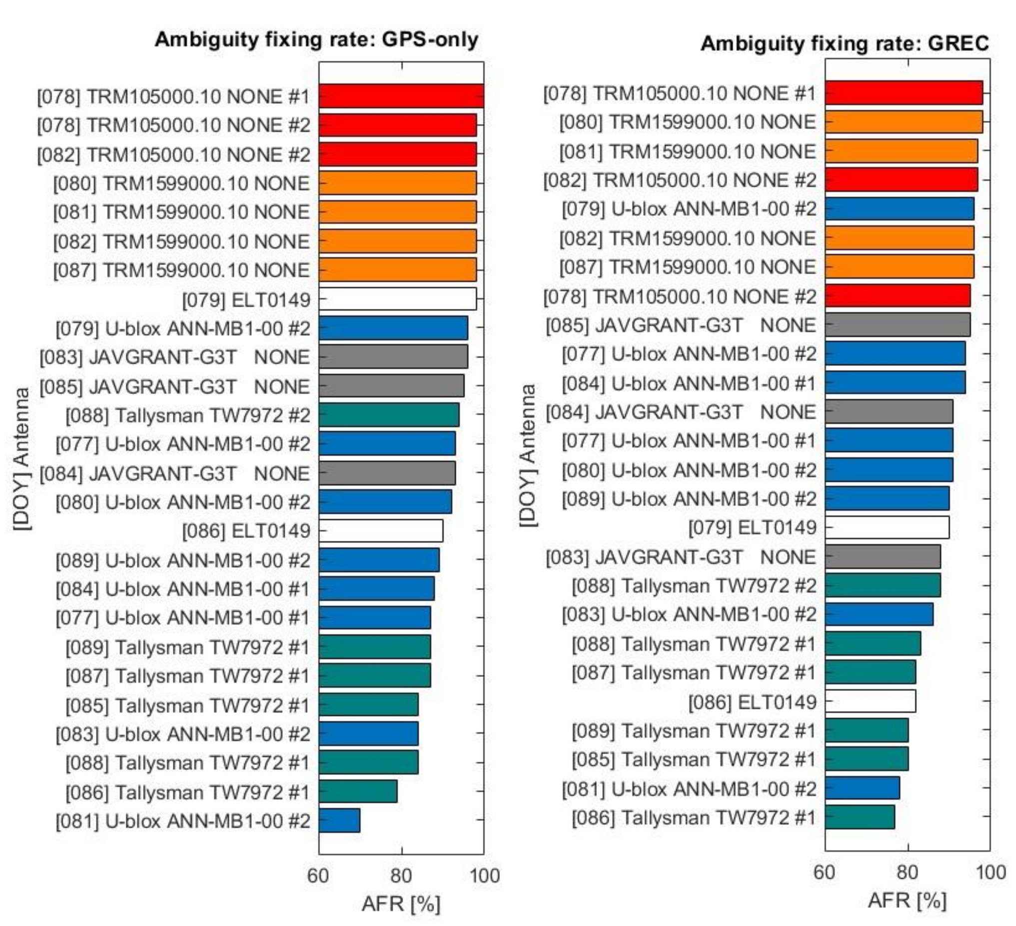

Fig. 3. Ambiguity fixing rates for G and GREC solutions.

Ambiguity resolution performance

Rates of fixed ambiguities (AFR) drop significantly for low-cost antennas compared to geodetic ones, often below 90% (Fig. 3). The AFRs obtained when using the TRM105000.10 and TRM159900.00 geodetic antennas are higher than 96%. AFR for the JAVGRANT-G3T antenna exceeds 91% for the GPS-only solution. For GREC it is slightly lower, which we associate with the problems in recording Beidou signals described in the section on the number of recorded observations for individual antennas and GNSS systems. For low-cost antennas, most AFR values fit the 80–90% range. The lowest AFR values were obtained on March 22, 2022 (DOY 81), for the U-blox ANN-MB-00 antenna. Then AFR equaled 70% and 78% for GPS-only and quadruple-system solutions, respectively. On March 27, 2022 (DOY 86) AFR for the Tallysman TW7972 equaled 79% and 77% for GPS-only and quadruple-system solutions, respectively. In comparison, on March 22, 2022, when using the TRM159900.00 antenna, the AFR reached 98% and 97%, respectively. When evaluating ambiguity resolution performance, we discovered no advantage of the Tallysman TW7972 antenna having a PCC model from calibration over the other low-cost antennas. In order to check the effect of PCO/PCC corrections on AFR, we once again performed processing observations without using these corrections. Slightly fewer zero difference ambiguities were detected without corrections but ultimately the single-difference AFR was mostly the same. In the case of the Tallysman and geodetic-grade antennas neglecting PCC in the GREC solution, there were isolated instances of fixing one less narrow-lane ambiguity resulting in a 1% reduction in AFR. Therefore, it can be concluded that the lack of PCO/PCC corrections has a marginal effect on AFR, and the lower values of this parameter in our study are mainly due to the quality and design of the antennas.

Tab. 4. Standard deviations of coordinate residuals from PPP-AR kinematic solutions.

		Mounting point #1					
		G			GREC		
		STD [mm]			STD [mm]		
DOY	Antenna	E	N	U	E	N	U
077	U-blox ANN-MB-00 #1	10.1	12.4	26.1	6.2	6.8	17.2
078	TRM105000.10 NONE #1	6.4	8.7	18.9	3.9	5.2	14.2
079	U-blox ANN-MB-00 #2	8.3	11.6	25.4	5.2	6.0	16.4
080	U-blox ANN-MB-00 #2	8.3	11.4	24.5	5.5	5.9	14.0
081	U-blox ANN-MB-00 #1	16.8	14.0	39.7	7.3	7.2	19.7
082	TRM105000.10 NONE #1	7.4	9.7	17.4	5.3	6.6	10.4
083	U-blox ANN-MB-00 #2	14.8	13.0	34.8	6.2	8.3	18.5
084	U-blox ANN-MB-00 #1	10.0	12.0	31.1	5.7	7.4	17.8
085	Tallysman TW7972 #1	11.7	12.3	29.0	6.9	7.0	23.7
086	Tallysman TW7972 #1	10.2	12.9	31.3	6.6	8.1	23.2
087	Tallysman TW7972 #1	11.8	12.8	32.3	7.9	9.0	15.8
088	Tallysman TW7972 #1	11.1	12.9	28.9	6.5	8.8	20.5
089	Tallysman TW7972 #1	10.6	13.2	32.2	6.2	7.1	16.8
		Mounting point #2					
DOY	Antenna	E	N	U	E	N	U
077	U-blox ANN-MB-00 #2	9.5	11.8	24.9	6.2	6.5	18.3
078	TRM105000.10 NONE #2	7.7	9.1	21.2	4.2	5.2	13.7
079	ELT0149	11.0	18.4	27.1	7.0	8.1	21.4
080	TRM159900.00 NONE	5.3	6.9	12.4	4.1	4.2	9.9
081	TRM159900.00 NONE	5.4	7.4	11.9	4.1	4.9	7.3
082	TRM159900.00 NONE	6.0	8.6	13.7	4.7	6.4	8.3
083	JAVGRANT-G3T NONE	9.6	10.7	23.2	5.4	6.8	15.4
084	JAVGRANT-G3T NONE	10.5	13.1	24.1	5.3	7.3	20.4
085	JAVGRANT-G3T NONE	8.5	13.0	21.4	5.9	7.2	15.3
086	ELT0149	12.8	17.5	37.4	9.0	12.0	21.1
087	TRM159900.00 NONE	5.2	7.2	13.1	3.5	5.0	9.4
088	Tallysman TW7972 #2	10.2	13.1	24.3	7.1	8.9	23.6
089	U-blox ANN-MB-00 #2	11.4	13.7	31.5	6.4	7.4	19.0
		Mean values					
	Antenna	E	N	U	E	N	U
	U-blox ANN-MB-00	11.2	12.5	29.8	6.1	6.9	17.6
	Tallysman TW7972	10.9	12.9	29.7	6.9	8.2	20.6
	ELT0149	11.9	18.0	32.3	8.0	10.1	21.3
	TRM159900.00 NONE	5.5	7.5	12.8	4.1	5.1	8.7
	TRM105000.10 NONE	7.2	9.2	19.2	4.5	5.7	12.8
	JAVGRANT-G3T NONE	9.5	12.3	22.9	5.5	7.1	17.0

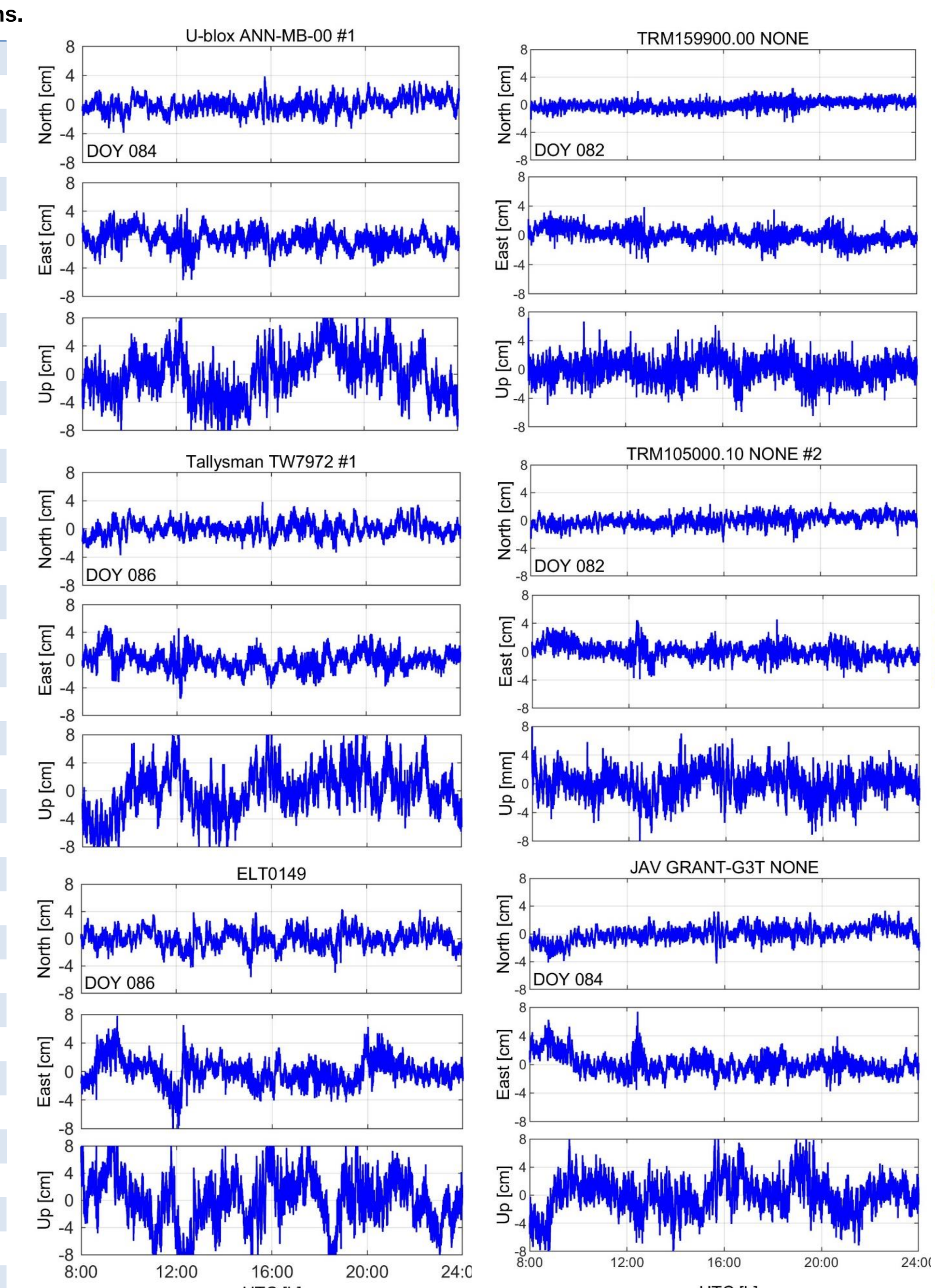

Fig. 4. Coordinate residuals time series of GPS-only PPP-AR kinematic solution for low-cost and high-grade antennas.

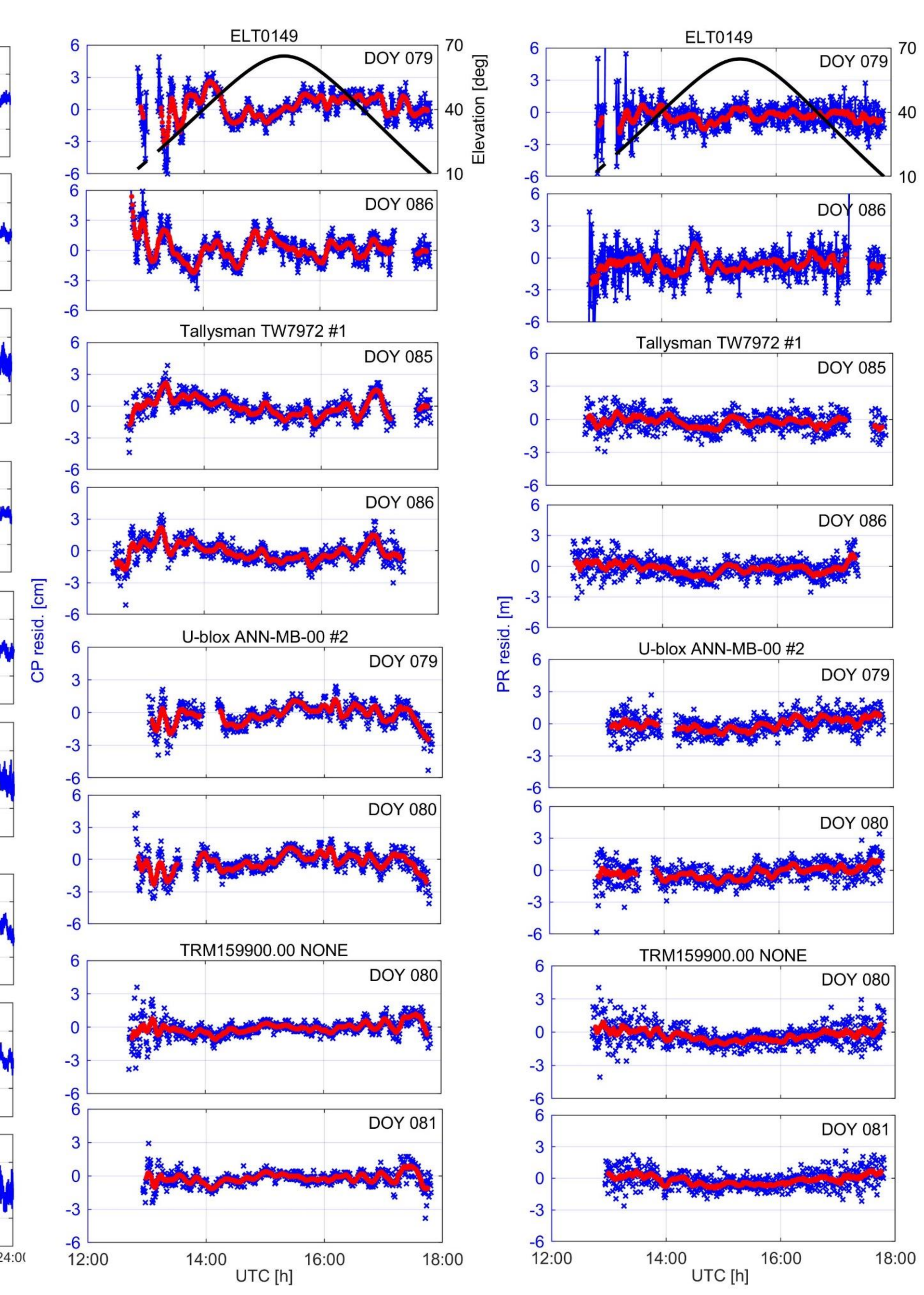

Fig. 5. Carrier phase and pseudorange IF residuals and elevation angle for GPS PRN 26 satellite for three tested low-cost antennas and high-grade TRM159900.00 one.

Kinematic positioning performance

The values of the standard deviation clearly separate geodetic antennas from the low-cost ones (Tab. 4, Fig. 4). In the case of the GPS-only solution for low-cost antennas, almost all coordinate error standard deviations exceed 10 mm or 20 mm in the horizontal and vertical planes, respectively. The situation is significantly improved when including observations from all GNSS systems. In the case of mass-market antennas, almost all standard deviations of the horizontal components drop to a level below 10 mm. For the vertical component, when using Tallysman TW7972 or ELT0149 antennas, only a few STDs exceed the adopted 20 mm threshold.

The results also reveal the significant benefit of using multi-constellation signals on precision in the kinematic solution for all antennas, from 3% up to 58% and about 40% on average. Such an effect is obtained, although even if antenna phase center corrections are provided, they are available only for GPS and GLONASS constellations. Kinematic PPP-AR highlights the divergences between high-grade and low-cost equipment as low-budget antennas provided the solutions with at least 1.5 times higher coordinate standard deviation compared to geodetic antennas.

Carrier phase and pseudorange IF residuals

The plot of CP residuals (Fig. 5) shows the repeatability of the plot shape for consecutive days from the processing using low-cost antennas, as well as greater fluctuation, which corresponds to lower positioning accuracy. Additionally, there are gaps in the recorded observations for the ELT0149 and U-blox ANN-MB-00 antennas. TRM159900.00, as expected, has the smallest residual variation. Conclusions from the analysis of PR residuals are similar, although the differences between Tallysman TW7972 and U-blox ANN-MB-00 and reference TRM159900.00 antenna are smaller than for CP residuals.

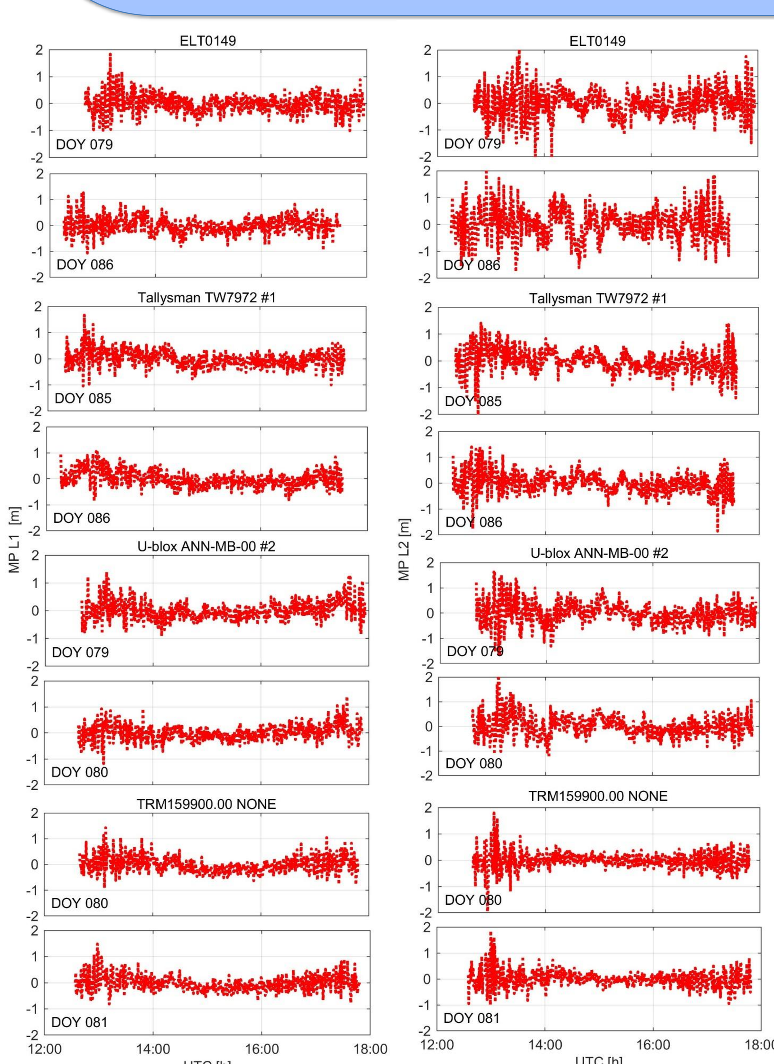

Fig. 6. Multipath of L1 and L2 from CMC linear combination for GPS PRN 26 satellite for the low-cost antennas and TRM159900.00.

Tab. 5. RMS of MP from CMC for different frequencies of GPS.

DOY	Antenna	RMS of MP for frequency [m]		Antenna	RMS of MP for frequency [m]	
	Mounting point #1	L1	L2	Mounting point #2	L1	L2
077	U-blox ANN-MB-00 #1	0.33	0.49	U-blox ANN-MB-00 #2	0.34	0.56
078	TRM105000.10 NONE #1	0.28	0.37	TRM105000.10 NONE #2	0.30	0.38
079	U-blox ANN-MB-00 #2	0.32	0.50	ELT0149	0.33	0.60
080	U-blox ANN-MB-00 #2	0.31	0.50	TRM159900.00 NONE	0.30	0.32
081	U-blox ANN-MB-00 #1	0.32	0.58	TRM159900.00 NONE	0.29	0.32
082	TRM105000.10 NONE #1	0.28	0.37	TRM159900.00 NONE	0.29	0.32
083	U-blox ANN-MB-00 #2	0.32	0.63	JAVGRANT-G3T NONE	0.31	0.44
084	U-blox ANN-MB-00 #1	0.33	0.51	JAVGRANT-G3T NONE	0.31	0.44
085	Tallysman TW7972 #1	0.31	0.49	JAVGRANT-G3T NONE	0.31	0.44
086	Tallysman TW7972 #1	0.31	0.49	ELT0149	0.35	0.64
087	Tallysman TW7972 #1	0.31	0.49	TRM159900.00 NONE	0.30	0.32
088	Tallysman TW7972 #1	0.31	0.49	Tallysman TW7972 #2	0.34	0.53
089	Tallysman TW7972 #1	0.31	0.49	U-blox ANN-MB-00 #2	0.34	0.63

Tab. 6. RMS of MP from CMC for different frequencies of Galileo.

DOY	Antenna	RMS of MP for frequency [m]		Antenna	RMS of MP for frequency [m]	
	Mounting point #1	E1	E5a	Mounting point #2	E1	E5a
077	U-blox ANN-MB-00 #1	0.32	0.40	U-blox ANN-MB-00 #2	0.33	0.44
078	TRM105000.10 NONE #1	0.28	0.27	TRM105000.10 NONE #2	0.29	0.30
079	U-blox ANN-MB-00 #2	0.31	0.41	ELT0149	0.34	0.50
080	U-blox ANN-MB-00 #2	0.32	0.43	TRM159900.00 NONE	0.22	0.19
081	U-blox ANN-MB-00 #1	0.33	0.45	TRM159900.00 NONE	0.20	0.18
082	TRM105000.10 NONE #1	0.27	0.27	TRM159900.00 NONE	0.21	0.19
083	U-blox ANN-MB-00 #2	0.33	0.50	JAVGRANT-G3T NONE	0.31	0.35
084	U-blox ANN-MB-00 #1	0.33	0.42	JAVGRANT-G3T NONE	0.29	0.34
085	Tallysman TW7972 #1	0.34	0.44	JAVGRANT-G3T NONE	0.32	0.37
086	Tallysman TW7972 #1	0.32	0.42	ELT0149	0.39	0.54
087	Tallysman TW7972 #1	0.33	0.43	TRM159900.00 NONE	0.20	0.18
088	Tallysman TW7972 #1	0.33	0.43	Tallysman TW7972 #2	0.34	0.52
089	Tallysman TW7972 #1	0.32	0.43	U-blox ANN-MB-00 #2	0.35	0.48

Multipath impact

The plots (Fig. 6) confirm the presence of multipath effect at the site as well as the significant susceptibility of the low-cost antennas to the multipath for low-elevated satellites. Noticeably, the plot is heavily scattered for low-elevation angles, particularly for the ELT0149 antenna. The results from the Tallysman TW7972 and the U-blox ANN-MB-00 are more similar to those from the TRM159900.00 antenna. However, a much larger fluctuation for higher elevation angles for the low-cost antennas can be seen. This regularity is even more evident in the case of the L2 frequency. In the case of the L1 GPS frequency (Tab. 5), the differences in the RMS of MP values are small. All values are close to 0.3 m, slightly favoring Trimble professional antennas. For L2 GPS, the differences in RMS of MP values are already much more noticeable- for U-blox ANN-MB-00 and ELT0149 antennas, the RMS of MP exceeds 0.60 m in some cases, and for Tallysman TW7972, it is slightly lower, amounting to 0.49-0.53 m. At the same time, these values for professional antennas range from 0.32–0.38 m for Trimble antennas L2 GPS and 0.44 m for JAVGRANT-G3T L2 GPS. We also note that the results obtained for different units of the same antenna type for consecutive days agree well.

For Galileo E1 frequency (Tab. 6), the results are similar to those of GPS L1. The exceptions are the results for the TRM159900.00 reference antenna, for which the RMS of MP values are between 0.20 and 0.22 m. Even better results, below the 0.2 m value, were obtained for this antenna at E5a frequencies. Values close to 0.30 m characterized the E5a RMS of MP values for the TRM105000.10 antenna, 0.35 m for JAVGRANT-G3T, and among the low-cost antennas 0.4-0.5 m for U-blox ANN-MB-00 and Tallysman TW7972 and above 0.5 m for ELT0149. As a result, the RMS of MP for low-cost antennas are often more than double those for Trimble choke-ring antenna.

Analyzing the results for low-cost antennas only, it can be concluded that the ELT0149 antenna is the most susceptible to MP among the tested ones. The best results among the low-cost antennas are achieved for the Tallysman TW7972 antenna, which is reflected in the lowest RMS of MP values, although they are only marginally better than U-blox ANN-MB-00. Compared to professional high-grade antennas, the RMSs of MP for low-cost ones are higher, from a few percent to twice, depending on the model and signal.

General summary and conclusions

We conclude that when using low-cost antennas for precise geodetic applications, one should expect at least a twofold decrease in positioning accuracy. To some extent, such an effect may be overcome when using signals from multiple satellite systems. However, it should be noted that this accuracy may drop even further in a multipath environment due to the susceptibility of low-cost antennas to this effect. We also report noticeable differences in positioning performance with different low-cost antennas that may be attributed to the completeness of the PCC models and antenna susceptibility to the multipath effect.

Acknowledgements

This study was supported by the project "Innovative precise monitoring system based on integration of low-cost GNSS and IMU MEMS sensors" POIR 01.01.01-00-0753/21, co-financed by the European Regional Development Fund within the Sub-measure 1.1.1 of the Smart Growth Operational Program 2014–2020. We would like to express our great appreciation for GNSS products, and the PRIDE PPP-AR software provided by Wuhan University.

The study was published in Krzan, G., Dawidowicz, K. & Paziewski, J. Low-cost GNSS antennas in precise positioning: a focus on multipath and antenna phase center models. GPS Solut 28, 103 (2024). https://doi.org/10.1007/s10291-024-01645-3